Biosensors and Bioelectronics 24 (2008) 638–643

Contents lists available at ScienceDirect

Biosensors and Bioelectronics

journal homepage: www.elsevier.com/locate/bios

Micro-machined piezoelectric membrane-based immunosensor array

Ting Xu [a], Zhihong Wang [a], Jianmin Miao [a,*], Ling Yu [b], Chang Ming Li [b]

[a] Micromachines Centre, Nanyang Technological University, 50 Nanyang Avenue, Singapore 639798, Singapore
[b] School of Chemical and Biomedical Engineering, Nanyang Technological University, Singapore 639798, Singapore

ARTICLE INFO

Article history:
Received 28 March 2008
Received in revised form 3 June 2008
Accepted 9 June 2008
Available online 21 June 2008

Keywords:
Biosensor
Piezoelectric membrane
Immunosensor array
Mass sensor

ABSTRACT

This paper reports a micro-machined piezoelectric membrane-based biosensor array for immunoassay. Goat immunoglobulin G (IgG) and HBsAg were immobilized as the probe molecules on the square piezoelectric membranes of the sensors that have dimensions of 3.5 μm × 500 μm × 500 μm. Due to the mass sensitive nature of these sensors, their resonant frequencies were depressed after the anti-goat IgG or anti-HBsAg was captured by the goat IgG or HBsAg. The resonant frequencies of the sensors were measured by an impedance analyzer. The experimental results demonstrate that the measured frequency change varies from 100 to 700 Hz, and the mass sensitivity of the device is estimated to be about 6.25 Hz/ng. A near linear relationship between the frequency change and the concentration of goat IgG was obtained, and the mass of the attached anti-goat IgG was calculated. The preliminary results discussed in this work indicate that the micro-machined piezoelectric membrane-based biosensor has a potential application as an immunosensor.

1. Introduction

A biosensor generally consists of a transducer and an affinity-based interface, which binds the biological receptors, and generates a detectable signal when the interested biological entities are captured. The transducer serves as sensor platform to detect the signal generated by the interface (Li et al., 2004).

Micro-machined piezoelectric biosensors are being widely investigated due to their many advantages over other sensors, such as compact size, high sensitivity, easy integration with an analysis circuit, and rapid response (Janshoff et al., 2000). Depending on the sensing platform of the sensor, micro-machined piezoelectric biosensors can mainly be classified into cantilever type, quartz-crystal micro-balance (QCM) type, and membrane type.

To date, micro-machined piezoelectric cantilever-based sensors (MPCS) are still the major player in the field of biosensing because of their high sensitivity and label free detection (Raiteri et al., 2001; Carrascosa et al., 2006). Most of these sensors use the mass micro-balancing technique to measure the change in resonant frequency after the capture of target molecules on a functionalized micro-cantilever surface (Hwang et al., 2004; Lee et al., 2006; Kang et al., 2006). However, MPCS suffers from a low quality merit factor (*Q* value), which makes it very difficult to be used in a liquid media. Furthermore, the fragility of these devices during fabrication processes and under real operating conditions also limits their extensive applications.

To overcome this issue, the QCM is developed as an alternative. Quartz has been successfully used in high sensitivity gas and liquid sensors for more than 30 years. Recently, QCM was reported to have successfully detected DNA and bacteria with good frequency stability and reproducibility (Mo et al., 2002; Mannelli et al., 2003). While this is a positive advancement, QCM remains unpractical for miniaturization and biosensor array application.

An interesting device based on micro-machined resonating piezoelectric membrane arrays was recently reported (Nicu et al., 2005). This device avoids problems, such as the fragility of the silicon-based cantilever in the micro-cantilever sensor and the lack of integration potential in the QCM biosensors. However, the affinity-based interface of this device is the open top surface of the membrane, and the reactive liquid that contains biomaterial can flow freely from one sensor to another sensor, resulting in undesired interaction between different biomaterials. Thus, this sensor array is not suitable for multi-biomaterial detection.

In this paper, we present another piezoelectric membrane-based biosensor array, which is fabricated with micro-machining techniques. This new device has a very compact size, relatively high sensitivity, rapid response, and it can be integrated with an analytical circuit easily. Additionally, this sensor array can detect multiple biological materials simultaneously because the interactions between the biomaterials take place within each reaction chamber. After characterization, it was verified that this sensor array can be used as an immunosensor. The working principle,

* Corresponding author. Tel.: +65 67906038; fax: +65 67924062.
E-mail address: mjmmiao@ntu.edu.sg (J. Miao).

0956-5663/$ – see front matter © 2008 Elsevier B.V. All rights reserved.
doi:10.1016/j.bios.2008.06.024

fabrication and characterization results will be introduced in the following section.

2. Mass sensitivity—theoretical analysis

The piezoelectric membrane-based biosensor presented here actually worked as a mass sensor. The working principle of this sensor is that the resonant frequency of the membrane decreases in response to a mass loading on the membrane surface. For an amount of mass added onto the micro-machined membrane surface, the resonant frequency change of the sensor is proportional to the added mass. The relationship is shown as follows:

$$\Delta f \propto \Delta m \tag{1}$$

where Δf denotes the frequency change, and Δm stands for the amount of mass added onto the device. The mass sensitivity S_M of a piezoelectric mass sensor can be defined as (Wenzel and White, 1989)

$$S_M = \lim_{\Delta M \to 0} \frac{\Delta f}{f_0} \frac{1}{\Delta M} \tag{2}$$

where ΔM is the mass per unit area loaded onto the surface of the sensor, and $\Delta f = f - f_0$ is the frequency change in response to the mass loading. The unit of S_M is m^2/kg. The resonant frequency of a thin square membrane with side width a can be expressed as

$$f_0 = \frac{\lambda_{ij}^2}{2\pi a^2} \sqrt{\frac{D}{\rho d}} = \frac{\lambda_{ij}^2}{2\pi a^2} \sqrt{\frac{D}{M}} \tag{3}$$

where $D = Ed^3/12(1-\nu^2)$ is the flexural rigidity, λ is a constant, ρ and d are the density and thickness of the membrane, respectively, and $M = \rho d$ is the mass per unit area of the membrane. Differentiating (3) with respect to M and using the definition (2), the mass sensitivity can be calculated as

$$S_M = \lim_{\Delta M \to 0} \frac{\Delta f}{f_0} \frac{1}{\Delta M} = -\frac{1}{2M} = -\frac{1}{2} \frac{1}{\sum_i \rho_i d_i} \tag{4}$$

where $M = \sum \rho_i d_i$ for the case of a multilayer membrane, and ρ_i and d_i are the density and thickness of the i^{th} layer of the membrane, respectively.

The fabricated membrane is simplified as a 3.5-μm-thick piezoelectric layer on a 1.8-μm-thick silicon oxide layer during the theoretical calculation. The densities of $Pb(Zr_{0.52}Ti_{0.48})O_3$ (PZT) and SiO_2 layers used for the simulation are 7.62×10^3 kg/m^3 and 2.07×10^3 kg/m^3, respectively (Yao et al., 2003). Based on Eq. (4), the theoretical mass sensitivity (S_M) of the fabricated sensor is calculated to be -16.5 m^2/kg.

An alternate definition of mass sensitivity is the resonant frequency change corresponding to a unit mass load (Thundat et al., 1995; Ilic et al., 2000). It can be written as

$$S_m = -\frac{\Delta f}{\Delta m} \tag{5}$$

where Δf is the frequency change due to an external introduced mass load Δm. The unit of S_m is Hz/kg. A larger absolute value of S_m means that the device is more sensitive.

Referring to Eqs. (3) and (4), the relationship between S_m and S_M can be rewritten as

$$S_m = -\frac{\Delta f}{\Delta m} = -\frac{f_0}{A} S_M \tag{6}$$

where f_0 is the resonant frequency before any mass is added to the membrane, S_M is the sensitivity in units of m^2/kg, and A is the area of the membrane. Since the dimensions and material properties of the membrane are constant, Eqs. (4) and (6) reveal that the sensitivity is already defined once the sensor is fabricated. The mass change is proportional to the detected frequency change and can be easily derived from Eq. (6) as

$$\Delta m = \frac{A}{S_M f_0} \Delta f \tag{7}$$

where f_0 is the resonance frequency which can be determined using impedance analysis due to the piezoelectric effect. S_M can be obtained from Eq. (4). Therefore, the mass of the biological entity captured by the bioreceptor is proportional to the resonance frequency change of the membrane, and thus can be calculated by measuring the resonant frequency change. This result is quite significant in quantitative mass analysis using such a sensor.

3. Micro-fabrication of the sensor array

3.1. Fabrication processes

The piezoelectric membrane-based biosensor array was fabricated using standard bulk micro-machining fabrication techniques. There were a total of 10 main steps involved. (1) A thermal silicon oxide layer (1.8 μm thick) was grown on a 4-in. double-sided polished silicon wafer. (2) A silicon nitride layer with a thickness of 200 nm and a lower temperature oxide (LTO) layer with a thickness of 350 nm were then deposited by low pressure chemical vapor deposition (LPCVD) on both sides of the wafer. (3) To open a window for backside silicon etching, the LTO and Si_3N_4/SiO_2 layers were etched by buffered oxide etching (BOE) and reactive ion etching (RIE). (4) After patterning, KOH wet etching was performed until the remaining thickness of silicon was about 50 μm. (5) Ti (20 nm)/Pt (200 nm) layers were sputtered, patterned on front side and used as bottom electrode. (6) PZT was used as the piezoelectric material for the membrane. A thick PZT layer with a required thickness of around 3.5 μm was deposited by the composite thick film deposition technique (Zhu et al., 2002; Wang et al., 2003). (7) Wet etching of the PZT in diluted HCl/HF solution was done to expose the bottom electrode pad. (8) A polyimide layer was spin-coated, patterned, and cured as an insulation layer to minimize parasitic capacitance induced by the patterned electrode wiring. (9) Ti (20 nm)/Pt (200 nm) layers were sputtered and patterned on the front side using lift-off to serve as the top electrode. (10) The backside silicon was etched away by KOH till the SiO_2 layer was exposed. (11) A layer of Au with thickness of 50 nm was sputtered on the surface of SiO_2 as the immobilization surface of the reaction chamber.

3.2. Fabrication results

Using the micro-machining process described above, the membrane-based piezoelectric biosensor array was successfully fabricated. As shown in Fig. 1(a), each array consists of seven individual sensors which are located in a hexagonal shape. Each square block shown in Fig. 1(a) is actually a single sensor. The fabrication of the device could obtain a very high yield due to the high quality thick PZT layer.

The backside of the array, which shows the reaction chambers, is illustrated in Fig. 1(b). The width of the sensor was about 0.51 mm, which was close to the designed value (0.5 mm). The opening area of the chamber was much larger than that of the bottom membrane due to the anisotropic wet etching by KOH. The subsequent biomaterial immobilizations processes, such as the dipping and washing of the biomaterial, were much more convenient due to this enlarged opening area.

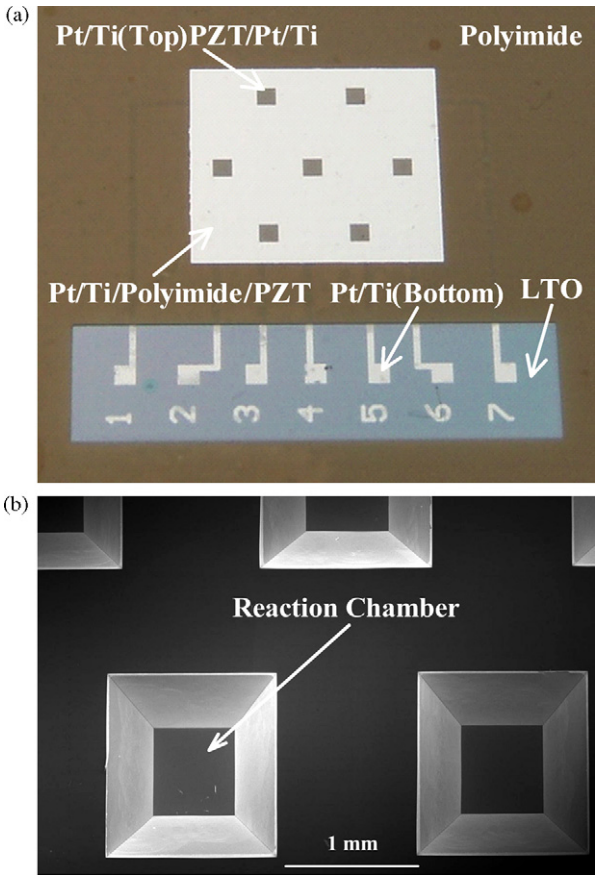

Fig. 1. Images of the fabricated sensor array: (a) optical image in top view; (b) SEM image of the reverse side.

4. Characterization

4.1. Biomaterial immobilization

The coupling effect between antigen and antibody is one of the most popular techniques for biosensing in immunosensor applications. The specific binding of the complementary species can be successfully detected with this approach. In this work, two different biological entities, goat immunoglobulin G (IgG) and HBsAg, were used to verify the feasibility of applying this sensor as an immunosensor.

The biological material immobilization was implemented by a dip and dry process (Ito et al., 1996), and the schematic process is shown in Fig. 2. Before the immobilization, a thin gold film (~50 nm) was sputtered onto the membrane in the reaction chamber. This thin metal surface will make the biomaterials immobilization easier (Lazcka et al., 2007; Ziegler et al., 1998). Biomolecules were immobilized onto the gold surfaces through the strong attachment between their native thiol functional groups (SH or SS) and Au (Arkady et al., 2000; Mirsky et al., 1997).

Goat IgG and HBsAg were immobilized onto the membrane surfaces to serve as receptors. Four individual sensors were immobilized with goat IgG in the first immobilization process. The reverse sides of the membranes that serve as sensing surfaces were firstly cleaned by acetone and isopropanol (IPA), and were dried out by nitrogen gas. Then 1 μl of goat IgG with different concentrations (Sigma, USA) in phosphate buffered saline (PBS, pH 7.4) was added into each reaction chamber. The concentrations of the added goat IgG for the four devices were 25 μg/ml, 50 μg/ml, 100 μg/ml, and 200 μg/ml, respectively. After 30 min of reaction at room temperature, the excess or unattached goat IgGs were washed away by carefully injected tris-buffered-saline (TBS washing buffer, pH 8.0). The goat IgG functionalized surfaces were dried under nitrogen flow. Because anti-goat IgG may directly attach onto the open gold surface between the goat IgGs and cause measurement inaccuracies, 1 μl of Blocker ™ Casein in TBS with a concentration of 1 mg/ml was dropped into each chamber to block the open surfaces.

The blockers and the goat IgG were again dried with nitrogen, and then the natural resonant frequencies of the four sensors were measured. Finally, in order to ensure a sufficient numbers of reactions between the goat IgG and anti-goat IgG, 1 μl of anti-goat IgG (Sigma, USA) with concentration of 100 μg/ml in PBS was added into each reaction chamber. After 30 min, the anti-goat IgGs were bonded with the immobilized goat IgGs, and the un-bonded anti-goat IgGs were washed away using TBS. After drying with nitrogen, the resonant frequencies were measured again. It can be seen that the total experimental time was less than 2 h, which was much faster than other reported times (Nicu et al., 2005; Lee et al., 2007) which typically took 7–12 h, or even longer to complete the process.

HBsAg was also immobilized on another sensor. The immobilization and washing process were the same as those for the previous four sensors. The concentrations for HBsAg (US Biological, USA), Blocker™ Casein, and anti-HBsAg (US Biological, USA) were 20 μg/ml, 1 mg/ml, and 200 μg/ml, respectively. To investigate the effect of washing processes on the sensors' resonant frequency, one sensor was used as the reference which underwent all the same washing and drying process, but no biomaterial was immobilized onto it.

In order to know the distribution of the captured anti-goat IgG, one reference sensor was immobilized with 1 μl of anti-goat IgG (25 μg/ml) labeled with Cy-3 in the last step. The fluorescent image of the captured anti-goat IgG could be observed using fluorescence microscopy with the images recorded by CCD camera

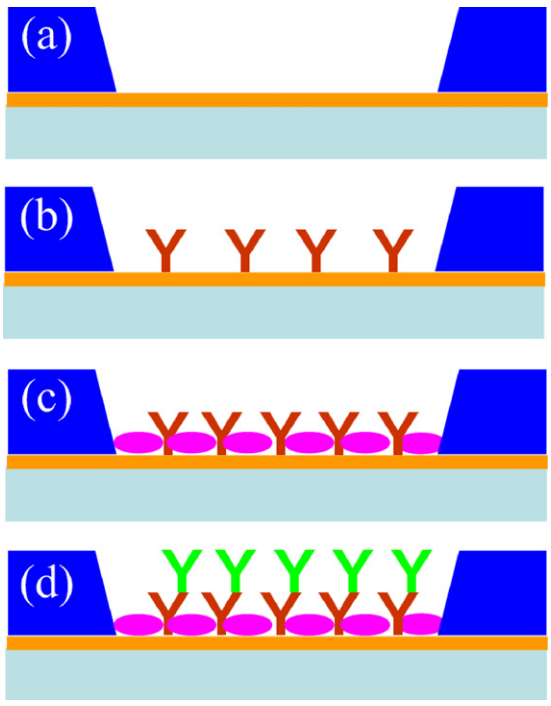

Fig. 2. Schematic processes of immobilizing goat IgG on the backside of the PZT membrane: (a) cleaning the backside of the membrane (with 50 nm thick Au layer); (b) attaching the goat IgG on to the Au surface; (c) blocking the open surface by Blocker™ Casein in TBS; (d) hybridization of goat IgG and anti-goat IgG.

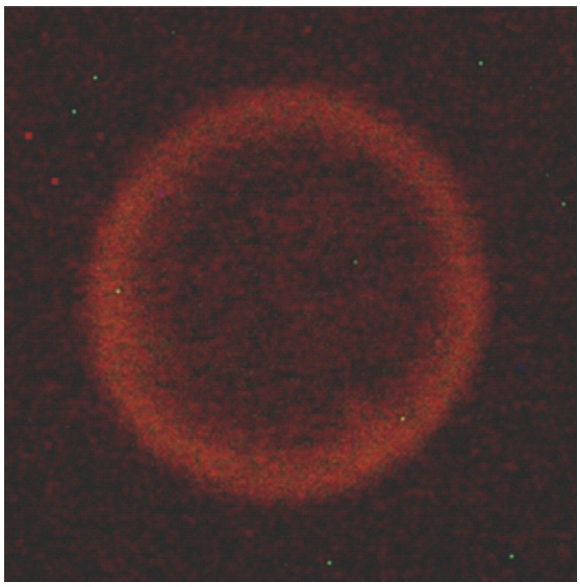

Fig. 3. Fluorescence image of one sensor after Cy-3 labeled anti-goat IgGs were absorbed.

(Nikon, Japan). The reaction chamber was totally black under the fluorescence microscopy before the anti-goat IgG was added.

4.2. Characterization results and discussion

Fig. 3 shows the pictures of the anti-goat IgGs (with Cy-3 label) distribution on the membrane of the reference sensor under a fluorescence microscope. The light dots clearly show that the labeled anti-goat IgGs were bonded with the goat IgGs. It can also be seen that the density at the edge of the membrane was higher than that in the center. This may have been caused by the drying and washing processes.

The piezoelectric membrane-based biosensors can be characterized using an impedance spectrum, which is one of the advantages of the piezoelectric biosensors. The Agilent 4294A impedance analyzer was used to test the fabricated biosensors. A probe station was used to connect the analyzer and the wiring pads of the sensors.

As the external biomaterials, such as goat IgG, HBsAg, and Blocker, were attached onto the sensing surfaces of the biosensors, the resonant frequencies of the sensors shift to the lower frequency domain. In order to study this relationship, the resonant frequency of the sensor was measured after each immobilization process was completed. The first reference resonant frequency (f_1) was measured after the thin gold layer was sputtered, and the second resonant frequency (f_2) was measured after the goat IgGs were immobilized. Hence, the first frequency shift was calculated as $\Delta f_1 = f_1 - f_2$. The resonant frequency after immobilizing blocker (f_3) and anti-goat IgGs (f_4) were subsequently measured. The last two frequency shifts were calculated as $\Delta f_2 = f_2 - f_3$ and $\Delta f_3 = f_3 - f_4$. All the measurements were conducted in gas phase with a temperature of 30 °C. Fig. 4(a) presents the frequencies of one sensor with a plain sensing surface (f_1), goat IgG and blocker (f_3), and anti-goat IgG (f_4). The frequency change varies from 100 to 700 Hz. The same measurement methods were also applied in the anti-HBsAg detecting processes. Fig. 4(b) shows the frequencies of another sensor with HBsAg, blocker, and anti-HBsAgs. Fig. 4 clearly shows that the frequency decreased after each type of biological entity was immobilized or adsorbed. The resonant frequencies of the sensors were measured at low frequency range (80–150 kHz), thus, the cost of measurement equipments are lower than that of high frequency measurement equipments. This is another merit of the sensors developed in this work.

Usually, during investigation of a calibration curve, probe molecular (Goat IgG in this work) with the same concentration is first immobilized on different sensors, whereas in the last step, the target molecular (anti-goat IgG) with different concentration is detected. Due to the limited binding sites in the immobilized goat IgG, if the concentration of the anti-goat IgG increases to a certain level, the redundant anti-goat IgG is not able to be captured by the goat IgG, hence a saturation adsorption occurs.

In this work, however, a different immobilizing process was used. Goat IgG was immobilized with different concentrations (25–200 μg/ml) in the first step; therefore, the numbers of goat IgG binding sites were proportional to the concentration of the solutions. In the last step, anti-goat IgG was applied onto the sensor surface with a relatively high concentration. This sufficiently high concentration of anti-goat IgGs ensures that all the binding sites in the goat IgGs were occupied by anti-goat IgGs. Due to the specific interaction between antigen and antibody, theoretically, the amount of the anti-goat IgGs captured by the goat IgG binding sites is proportional to the concentration of immobilized goat IgG. Therefore, a nearly linear relationship between the frequency shift (after anti-goat IgGs were captured) and the concentration of the immobilized goat IgG is expected.

The advantage of our immobilization method is that the capability of the new biosensors for the detection of added mass and performance uniformity can be proved after the first immobilization process. Based on Eq. (1), it can be seen that the resonant

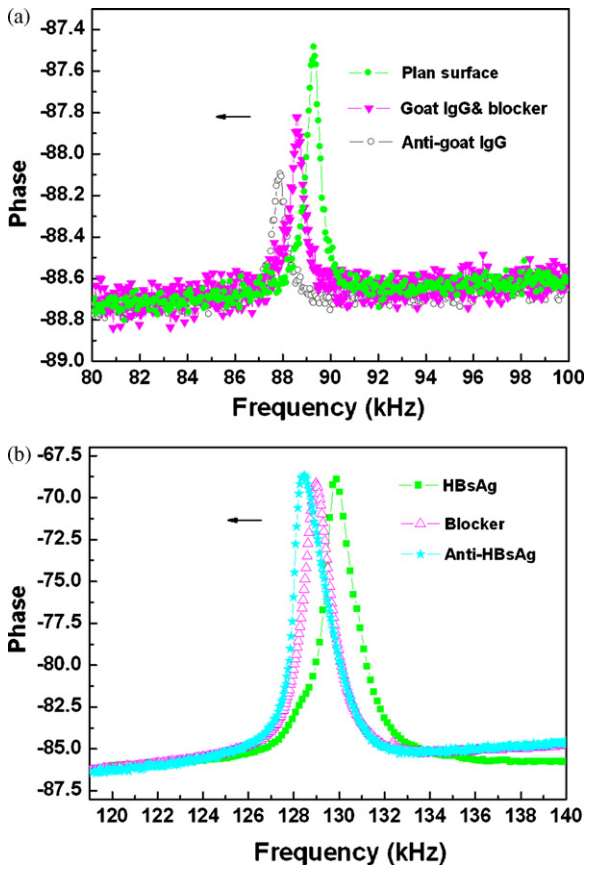

Fig. 4. Phase-frequency spectra of the sensors during each immobilization process: (a) frequency change of one sensor in response to immobilization of goat IgG and blocker and captured anti-goat IgGs; (b) frequency change of another sensor after HBsAg, blocker, and anti-HBsAgs were immobilized or captured.

frequency of the sensor should be changed after the external mass is added, and the frequency shift is proportional to the mass change. In this work, the added mass in the first step is actually the mass of the immobilized goat IgG which is proportional to the concentration of its solution. After the goat IgGs with concentrations of 25 μg/ml, 50 μg/ml, 100 μg/ml, and 200 μg/ml were immobilized on the four different sensors, the frequency shifts were measured to be 150 Hz, 258 Hz, 530 Hz, and 1100 Hz, respectively. The frequency shift is nearly proportional to the concentration of immobilized goat IgG, indicating that the sensor array is mass sensitive and the performances of the sensors are reasonably uniform. After the mass sensitive feature of the sensor array was confirmed, we further evaluated the immunoassay performances of the array by applying the anti-goat IgG.

The dose/signal curve was plotted in Fig. 5(a), the frequency shifts were calculated based on the average frequency values after five measurements. In the tested goat IgG concentration range of 25–200 μg/ml, a nearly linear relationship between the frequency shift (after anti-goat IgGs were captured) and the concentration of goat IgG was found. This reveals that a higher concentration of goat IgG added onto the sensor in the first immobilization process will result in a larger frequency shift after capturing the anti-goat IgG in the last step. This is mainly because of more goat IgG binding sites were available in higher concentration of immobilized goat IgG to capture anti-goat IgGs.

The resonant frequencies of the reference sensors have negligible variations (<50 Hz) during the washing process. This reveals that washing process has a negligible effect on the sensor's frequency. This also indicates that nonspecific adsorption is not significant in this immobilization processes.

The mass of the captured anti-goat IgG in the last process can be calculated by Eq. (7). The surface area (A) is 2.5×10^{-7} m^2 (500 μm × 500 μm), and S_M is −16.5 m^2/kg. The reference frequency (f_0) in the equation was measured after the blocker was immobilized. Frequency change (Δf) was calculated as $\Delta f_3 = f_3 - f_4$. The calculated masses adsorbed by the four sensors are 16.1 ng, 52.3 ng, 78.2 ng, and 108 ng, respectively. The linear relationship between the calculated mass and the frequency change is presented in Fig. 5(b). This result is well consistent with the conclusion from Eq. (7), and it justifies that the performances of the sensors in this array were quite uniform. From the gradient of Fig. 5(b), the average mass sensitivity of these four sensors was calculated to be 6.25 Hz/ng. This result proves that the sensor array developed in this work can detect the mass of the biomaterials in quantity.

The mass of the immobilized blocker can also be calculated by Eq. (7), and it was much smaller than that calculated by the added concentration and volume. This reveals that the majority of the sensor surfaces were occupied by the goat IgG and there were not many open surfaces for the blockers to attach onto. Hence, it can be concluded that the mass change in the last step was mainly due to the captured anti-goat IgG. This ensures the accuracy of the anti-goat IgG detection. The primary results obtained in these experiments proved to be meaningful in the detection of small quantities of biomaterials.

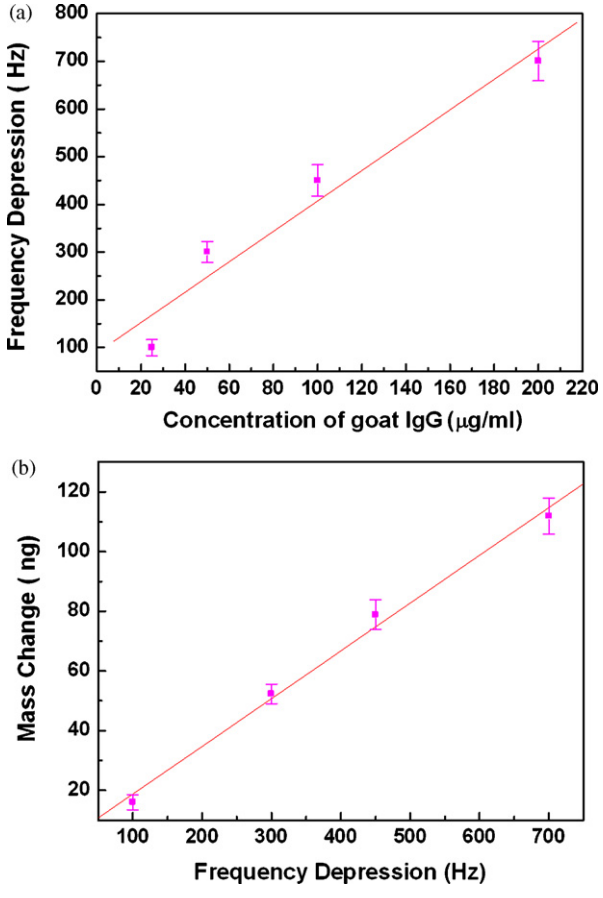

Fig. 5. Relationship between frequency depression, concentration of goat IgG, and mass change for four sensors in the same array: (a) relationship between the frequency depression and the concentration of goat IgG; (b) relationship between the mass change and frequency depression after the anti-goat IgGs were captured.

5. Conclusions

In this study, we presented a mass sensitive PZT membrane (3.5 μm thick)-based biosensor array for immunoassay applications. The array was fabricated by micro-machining techniques and consisted of seven individual sensors, which were 500 μm by 500 μm in dimension. Goat IgG and HBsAg were immobilized as probe molecules on the sensing membrane to capture the target biomolecule, anti-goat IgG and anti-HBsAg. The frequency changes were electrically measured by an impedance analyzer. The mass sensitivity of the device was estimated to be about 6.25 Hz/ng for detection of anit-goat IgG. The primary results indicate that micro-machined piezoelectric sensor array has the feasibility for immunosensor applications. With further improvement and calibration in the future, the sensor array can simultaneously detect either multiple biological entities or the same biological entity with different concentrations. Therefore, it has the potential to be applied in a disposable biochip for rapid and low cost medical diagnosis or food quality monitoring.

Acknowledgment

The authors acknowledge the financial support from the Center for Advanced Bionanosystems, Nanyang Technological University.

References

Arkady, A.A., Presnova, V., Rubtsova, M., Egorov, A.M., 2000. Analytical Chemistry 72, 3805–3811.
Carrascosa, L.G., Moreno, M., Alvarez, M., Lechuga, L.M., 2006. Trends in Analytical Chemistry 25, 196–206.
Hwang, K.S., Lee, J.H., Park, J., Yoon, D.S., Park, J.H., Kim, T.S., 2004. Lab Chip 4, 547–552.
Ilic, B., Czaplewsli, D., Craighead, H.G., Neuzil, P., Campagnolo, C., Batt, C., 2000. Applied Physics Letters 77, 450–452.
Ito, K., Hashimoto, K., Ishimori, Y., 1996. Analytical Chimica Acta 327, 29–35.
Janshoff, A., Galla, H.J., Steinem, C., 2000. Angewandte Chemie-International Edition 39, 4004–4032.
Kang, G.Y., Han, G.Y., Kang, J.Y., Cho, I.H., Park, H.H., Paek, S.H., Kim, T.S., 2006. Sensors and Actuators B: Chemical 117, 332–338.

Lazcka, O., Campo, F.J.D., Muñoz, F.X., 2007. Biosensors & Bioelectronics 22, 1205–1217.
Lee, K.H., Su, Y.D., Chen, S.J., Tseng, F.G., Lee, G.B., 2007. Biosensors and Bioelectronics 23, 466–472.
Lee, Y., Lim, G., Moon, W., 2006. Sensors and Actuators A: Physical 130, 105–110.
Li, S., Li, Z., Chin, B.B., Cheng, Z.Y., 2004. Proceedings of SPIE 5389, 306–313.
Mannelli, I., Minunni, M., Tombelli, S., Mascini, M., 2003. Biosensors & Bioelectronics 18, 129–140.
Mirsky, V.M., Riepl, M., Wolfbeis, O.S., 1997. Biosensors & Bioelectronics 12, 977–989.
Mo, X.T., Zhou, Y.P., Lei, H., Deng, L., 2002. Enzyme Microbial Technology 30, 583–589.
Nicu, L., Guirardel, M., Chambosse, F., Rougerie, P., Hinh, S., Trevisiol, E., Francois, J.M., Majoral, J.P., Caminade, A.M., Cattan, E., 2005. Sensors and Actuators B: Chemical 110, 125–136.
Raiteri, R., Grattarola, M., Butt, H.J., Skladal, P., 2001. Sensors and Actuators B: Chemical 79, 115–126.
Thundat, T., Wachter, E.A., Sharp, S.L., Warmack, R.J., 1995. Applied Physics Letters 66, 1695–1697.
Wang, Z., Zhu, W., Zhao, C., Tan, O.K., 2003. Materials Science and Engineering B 99, 56–62.
Wenzel, S.W., White, R.M., 1989. Applied Physics Letters 54, 1976–1978.
Yao, L.Q., Lu, L., Wang, Z.H., Zhu, W.G., Dai, Y., 2003. IEEE Transactions on Ultrasonics, Ferroelectrics, and Frequency Control 50, 1262–1271.
Zhu, W., Wang, Z., Zhao, C., Tan, O., Hng, H., 2002. Japanese Journal of Applied Physics 41, 6969–6975.
Ziegler, Z., Gopel, W., Hammerle, H., Hatt, H., Jung, G., Laxhuber, L., Schmidt, H.L., Schutz, S., Vogtle, F., Zell, A., 1998. Biosensors and Bioelectronics 13, 539–571.